JOURNAL OF VIROLOGY, June 1995, p. 3658–3667 Vol. 69, No. 6
0022-538X/95/$04.00+0


# Interaction between the 5′-Terminal Cloverleaf and 3AB/3CD$^{pro}$ of Poliovirus Is Essential for RNA Replication

WENKAI XIANG, KEVIN S. HARRIS,† LOUIS ALEXANDER,‡ AND ECKARD WIMMER*

*Department of Molecular Genetics and Microbiology, School of Medicine, State University of New York at Stony Brook, Stony Brook, New York 11794-5222*

Received 8 December 1994/Accepted 7 March 1995

**On the basis of sequence alignments and secondary structure comparisons of the first 100 nucleotides of enterovirus and rhinovirus RNAs, chimeric constructs in which this region of poliovirus type 1 Mahoney [PV1(M)] is replaced with that of human rhinovirus type 2 (HRV2) or HRV14 have been engineered. These chimeric constructs contain the internal ribosomal entry site of either poliovirus or encephalomyocarditis virus. Independent of the internal ribosomal entry site elements, only the constructs containing either the PV1(M) or HRV2 cloverleaf sequences yielded viable viruses. The secondary structures of all three cloverleaves are quite similar. However, highly purified polioviral proteins 3CD$^{pro}$ and 3AB together bound to the PV1(M) and HRV2 cloverleaves, albeit with different affinities, whereas the HRV14 homolog did not interact with these proteins to any appreciable extent. These results support a mechanism of poliovirus genomic replication in which the formation of a complex between the cloverleaf structure and the 3CD$^{pro}$/3AB proteins of poliovirus plays an essential role.**

Two genera in the family *Picornaviridae*, *Enterovirus* and *Rhinovirus*, are known to be closely related with respect to their structure and genome organization (30). This kinship also applies to the sequences of the 5′ nontranslated regions (NTRs) of the human pathogens polioviruses (causing poliomyelitis) and rhinoviruses (causing the common cold) (24, 25, 28).

Poliovirus genomic RNA possesses a 5′ NTR (Fig. 1A) that is unusually long for RNA viruses, a characteristic common to all picornaviruses. This region bears important *cis*-acting elements for viral proliferation. The first 100 nucleotides (nt) of poliovirus genomic RNA form a characteristic cloverleaf-like structure (Fig. 1A and Fig. 2) (3, 15, 28). Manipulations that affect this structure can be lethal or can result in replication phenotypes (3, 26, 29, 33). Amongst enteroviruses and rhinoviruses, the level of sequence conservation of the first 100 nt is high (≈70%). Moreover, human rhinovirus type 2 (HRV2) and HRV14, two representatives of the genus *Rhinovirus*, can form cloverleaf structures very similar to that of poliovirus (Fig. 2A and B) (28). The conservation of the sequences and structures implies functional importance of these elements.

A second genetic element within the 5′ NTR, the internal ribosomal entry site (IRES), is essential for the initiation of cap-independent polyprotein synthesis (10, 11, 22, 23, 35). The translation-coupled *cis* cleavages and the subsequent *trans* cleavages of the polyprotein by virally encoded proteinases yield the structural and nonstructural proteins (7, 16). Interestingly, some cleavage intermediates with relatively long half-lives attain functions distinct from those of their cleavage products (35). Recent studies have uncovered specific viral precursor proteins that are indispensable for both protein processing and RNA synthesis. The primary cleavage products, 3AB and 3CD$^{pro}$, of the P3 region are the striking examples to support this observation. 3AB is the precursor of VPg, and 3CD$^{pro}$ is a proteinase as well as the precursor for the RNA polymerase 3D$^{pol}$. These two proteins, which map next to each other in the viral genome (Fig. 1B), form a complex in solution (17). This interaction may already exist in the P3 precursor, although the latter is very rapidly processed (7, 16).

Andino et al. (3, 4) first provided genetic and biochemical evidences that poliovirus 3CD$^{pro}$ has the propensity to bind to the poliovirus cloverleaf, if a cellular protein ("host factor") of unknown structure (p36) is present to assist binding. Recently, Harris et al. (9) have reported that a proteolytic cleavage product (p36) of the eukaryotic elongation factor EF-1α (50 kDa), a protein found abundantly in the cell cytoplasm, can promote the binding of poliovirus 3CD$^{pro}$ to the cloverleaf. Harris et al. (9) also provided evidence that the host factor can be replaced with 3AB, that is, that the naturally occurring complex 3AB/3CD$^{pro}$, but not purified 3CD$^{pro}$ alone, can bind to the cloverleaf RNA with high affinity.

We have substituted the cloverleaf of poliovirus type 1 Mahoney [PV1(M)] (region I in Fig. 1A) with the corresponding elements of either HRV2 or HRV14, while utilizing the IRES elements of either PV1 or encephalomyocarditis virus (EMCV) to promote translation (Fig. 3A). Amongst the wild-type and five chimeric genomes, only those containing either the PV1(M) or HRV2 cloverleaf supported polioviral RNA synthesis in an IRES-independent manner. Indeed, these chimeric RNAs generated viable viruses. In contrast, constructs containing the HRV14 cloverleaf expressed a null phenotype. Our data indicate that the apparent ability of the three cloverleaf entities to induce RNA replication correlated with the extent to which the poliovirus protein 3AB/3CD$^{pro}$ complex interacted with cloverleaf RNAs in vitro. It can, therefore, be concluded that the interaction between the poliovirus-specific proteins 3AB/3CD$^{pro}$ and the 5′ end of the genome is likely to be essential for RNA replication.

## MATERIALS AND METHODS

**Plasmid construction.** By site-directed mutagenesis (13), a unique *Sma*I site was introduced into nt 100 of PV1(M) cDNA in plasmid pT7PVM1 (6), which generated plasmid pT7PVMS100. To construct plasmid pP100ENPO, a frag-

* Corresponding author. Phone: (516) 632-8787. Fax: (516) 632-8891.

† Present address: Fred Hutchinson Cancer Research Center, Basic Science Division, Seattle, WA 98104.

‡ Present address: Harvard Medical School, New England Regional Primate Center, Southborough, MA 017722.

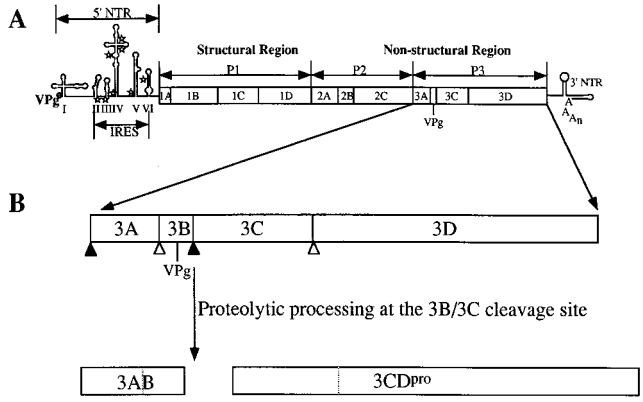


FIG. 1. Structure of poliovirus genomic RNA (modified from that presented in reference 9). (A) RNA domains in the 5′ NTR are indicated by Roman numerals. Domain I is the cloverleaf, whose 5′ end is covalently linked to VPg. Stars indicate the positions of noninitiating AUG triplets. The open box depicts the polyprotein with coding regions for different viral proteins. The 3′ NTR contains a pseudoknot and is polyadenylylated (for details, see reference 35). (B) Enlargement of the P3 nonstructural precursor. Closed and open triangles indicate rapidly and slowly processed Q/G cleavage sites, respectively.

ment from the *Sma*I site to the *Nhe*I site in pPVMS100 was switched with the one from the *Eco*RI site to the *Nhe*I site in pP108ENPO (1), which contains the EMCV IRES. pR2PIO, pR2ENPO, pR14PIO, and pR14ENPO were constructed by replacing the first 100 nt in PVMS100 or P100ENPO cDNA with either the first 98 nt in HRV2 cDNA or the first 97 nt in HRV14 cDNA. The pT7HRV2 plasmid was a generous gift from E. Kuechler. The pT7HRV14 plasmid was a generous gift from R. Rueckert.

**In vitro transcription and in vitro translation.** Prior to transcription with T7 RNA polymerase, template DNAs were linearized with *Eco*RI, an enzyme cleaving at a unique site close to the 3′ side of the cDNA poly(A) tracts. The conditions for the in vitro transcription have been previously described (34).

Equal amounts of RNA transcripts were used to program HeLa cell translation extracts (18). After incubation overnight at 30°C, aliquots of $^{35}$S-labeled samples were analyzed by electrophoresis on sodium dodecyl sulfate (SDS)–12.5% polyacrylamide gels followed by autoradiography.

**RNA transfection, plaque assay, and one-step growth curve.** All assays were performed with R19 HeLa cell monolayers maintained in Dulbecco modified Eagle medium supplemented with 2% bovine serum (GIBCO). RNA transfections were carried out by the DEAE-dextran method (12). Cell lysates harvested from transfected cells were subjected to plaque assay.

In viral one-step growth assays, HeLa cell monolayers ($10^6$ cells) were infected at a multiplicity of infection of 10. After 30 min of incubation at room temperature, the cells were washed with HBSS buffer (GIBCO) and incubated at 37°C with prewarmed medium. At various time points postinfection, the cells of duplicate plates were harvested and the titers of the viruses were determined by plaque assay.

**Detection of viral RNA synthesis.** To detect plus-strand RNA synthesis, HeLa cell monolayers ($2 \times 10^6$ cells) were transfected with one of six RNA transcripts, incubated at room temperature for 30 min, and washed twice with HBSS buffer, and then prewarmed medium was added. All steps from RNA extraction to hybridization were carried out according to the procedures previously described (21). Briefly, one-half of the extracted intracellular RNAs was used in the assay. A 386-nt riboprobe, complementary to the 3′ end of plus-strand RNA, was labeled with [$\alpha$-$^{32}$P]UTP and used for hybridization (27).

To detect minus-strand RNA synthesis, 1/10 of the RNA samples extracted from the cells at 0 or 23 h after transfection was treated with RNase-free DNase to eliminate DNA contamination and then preheated at 100°C for 5 min to separate the minus-strand RNA from the plus-strand RNA. By using primer 1 (5′ AGTCTGGTGCCCGCGTCCACC 3′; nt 3280 to 3300 of PVMS100 cDNA), the reverse transcription reactions were carried out with *Tth* polymerase at 70°C for 30 min, and then the products were digested with RNase A (10 $\mu$g) for 15 min at 37°C. The cDNAs were amplified by PCR using *Taq* polymerase with primer 1 and primer 2 (5′ CCTGAGTGGCCAAGTGGTAGTTGC 3′; complementary to nt 3435 to 3458 of PVMS100 cDNA). A total of 25 amplification cycles were performed, each cycle consisting of 45 s of denaturation at 94°C, 45 s of annealing at 60°C, and 1 min of polymerization at 72°C. (All the enzymes used in this assay were purchased from Boehringer Mannheim Co.)

**RNA binding assay.** RNA gel shift analyses were carried out as previously described (9); each reaction mixture contained 20,000 cpm of [$\alpha$-$^{32}$P]UTP-labeled PV1(M), HRV2, or HRV14 cloverleaf RNA. The binding buffer consisted of 5 mM MOPS (morpholinepropanesulfonic acid; pH 7.4), 25 mM KCl, 2 mM $MgCl_2$, 20 mM dithiothreitol, and 15 $\mu$g of tRNA from baker's yeast (Boehringer Mannheim). The final concentration of purified 3CD$^{pro}$ (a 3C/3D cleavage site mutant expressing only residual activity of autocleavage; see reference 8 for details) was kept constant at 0.2 $\mu$M, while that of purified 3AB ranged from 0.4 to 1.6 $\mu$M. RNAs 1A′B and 1A′BC (nt 1 to 34 and 1 to 45 of the polioviral genome, respectively) were expressed from pPN6-derived plasmids (plasmid pPN6 was a generous gift from R. Andino) (9). These RNAs, along with whole cloverleaf RNAs of PV1(M), HRV2, and HRV14, were used in competition experiments. Each of these RNA competitors was mixed with $^{32}$P-labeled cloverleaf RNA prior to addition to the binding reaction mixture.

**UV cross-linking assay.** A total of 200,000 cpm of [$\alpha$-$^{32}$P]UTP-labeled cloverleaf RNA was incubated with 3AB and/or 3CD$^{pro}$ under the conditions used for the RNA gel shift assays, and 15 $\mu$g of baker's yeast tRNA was added as a nonspecific competitor (approximately 1,000-fold molar excess over the cloverleaf RNA). The mixtures were then UV cross-linked by using UV Stratalinker 1800 for 30 min and subjected to RNase A (20 $\mu$g), $T_2$ (4 units), and $U_1$ (2 units) digestion. The products were analyzed by SDS–13% polyacrylamide gel electrophoresis (PAGE) and autoradiography.

## RESULTS

**Secondary structure comparison of the first 100 nt in PV1, HRV2, and HRV14 genomic RNA.** In comparison with the first 100 nt of the PV1 genome, there are 27 and 33 nucleotide differences within the same segments of the HRV2 and HRV14 genomes, respectively. However, the computer-predicted secondary structures in these three RNA sequences are very similar (28). The existence of this cloverleaf-like structure at the 5′ end of PV1 was confirmed by genetic and biochemical analyses (3, 15).

In the first 100 nt of HRV2 (Fig. 2A), 18 of 27 nt that differ from the PV1 sequence are located in stem regions. The lengths of stems A, B, and C are the same in both structures, but stem D of the HRV2 cloverleaf is shorter (because of a 2-nt deletion) than its PV1 counterpart. The eight nucleotide differences in the loop regions, however, have no effect on the loop sizes.

In the case of the HRV14 cloverleaf (Fig. 2B), 15 of 33 nucleotide differences are located in stem regions, leaving stems A, B, and D shorter than their PV1 counterparts. Thirteen nucleotide changes can be observed in the loop regions. Loops B and D are smaller than their PV1 counterparts by 2 and 1 nt, respectively. In total, there are more extensive structural differences between the first 100 nt of PV1 and HRV14 than between the first 100 nt of PV1 and HRV2.

The comparison of the two rhinovirus homologs (Fig. 2C) displayed an extent of difference similar to that observed between PV1 and HRV14: 20 of 33 nucleotide differences are located in stem regions, leaving stems A and B in HRV14 shorter than their HRV2 counterparts. Nine nucleotide changes can be observed in the loop regions; loops B and D in HRV14 are smaller than their HRV2 counterparts by 2 and 1 nt, respectively. Overall, the structures of the first 100 nt of PV1 and HRV2 are the most closely related among these three homologs.

**Plasmid construction and in vitro translation.** As illustrated in Fig. 3A, the six plasmid constructs all contained identical PV1(M) open reading frames (ORFs) and 3′ NTRs. However, the 5′-terminal cloverleaves of pPVMS100, pR2PIO, and pR14 PIO originated from PV1(M), HRV2, and HRV14, respectively. Plasmids pP100ENPO, pR2ENPO, and pR14ENPO were similar to the plasmids mentioned above except that the PV1 IRES was exchanged for the EMCV IRES. The integrity of each construct for the region of genetic changes was verified by DNA sequencing.

All plasmids were linearized with *Eco*RI and used as templates for transcription in vitro. HeLa cell extracts were programmed with equal amounts of transcript RNAs, a system that faithfully translates polioviral RNA in vitro with concomitant proteolytic processing resembling that observed in vivo

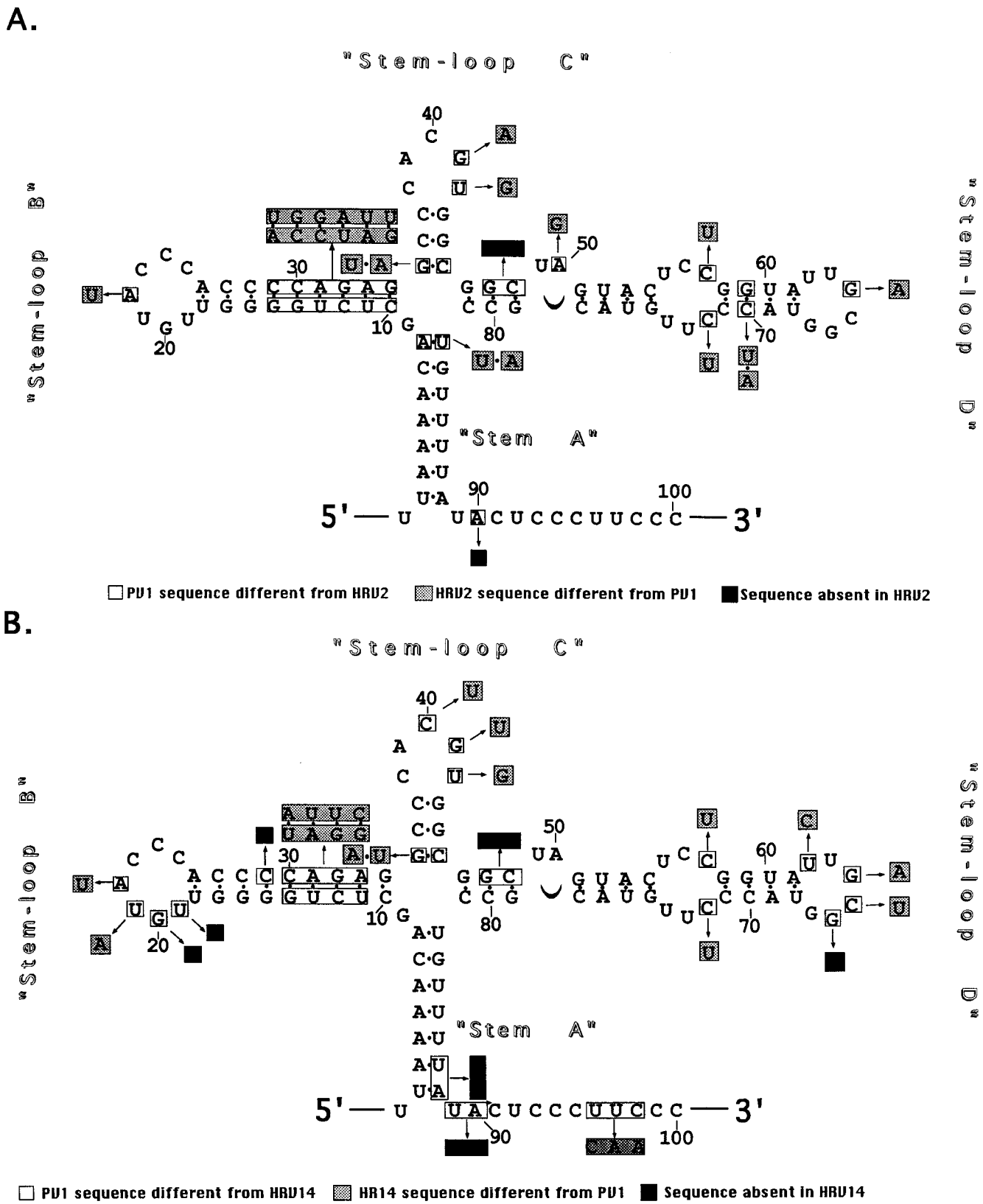


FIG. 2. Secondary structure comparisons of cloverleaf elements from PV1(M), HRV2, and HRV14. (A) Comparison of PV1(M) and HRV2 cloverleaves. The total number of nucleotides differing between them is 27, the number of nucleotides differing in stem regions is 18, and the number of nucleotides absent in HRV2 is 3. (B) Comparison of PV1(M) and HRV14 cloverleaves. The total number of nucleotides differing between them is 33, the number of nucleotides differing in stem regions is 15, and the number of nucleotides absent in HRV14 is 10. (C) Comparison of HRV2 and HRV14 cloverleaves. The total number of nucleotides differing between them is 33, the number of nucleotides differing in stem regions is 20, and the number of nucleotides absent in HRV14 is 7.

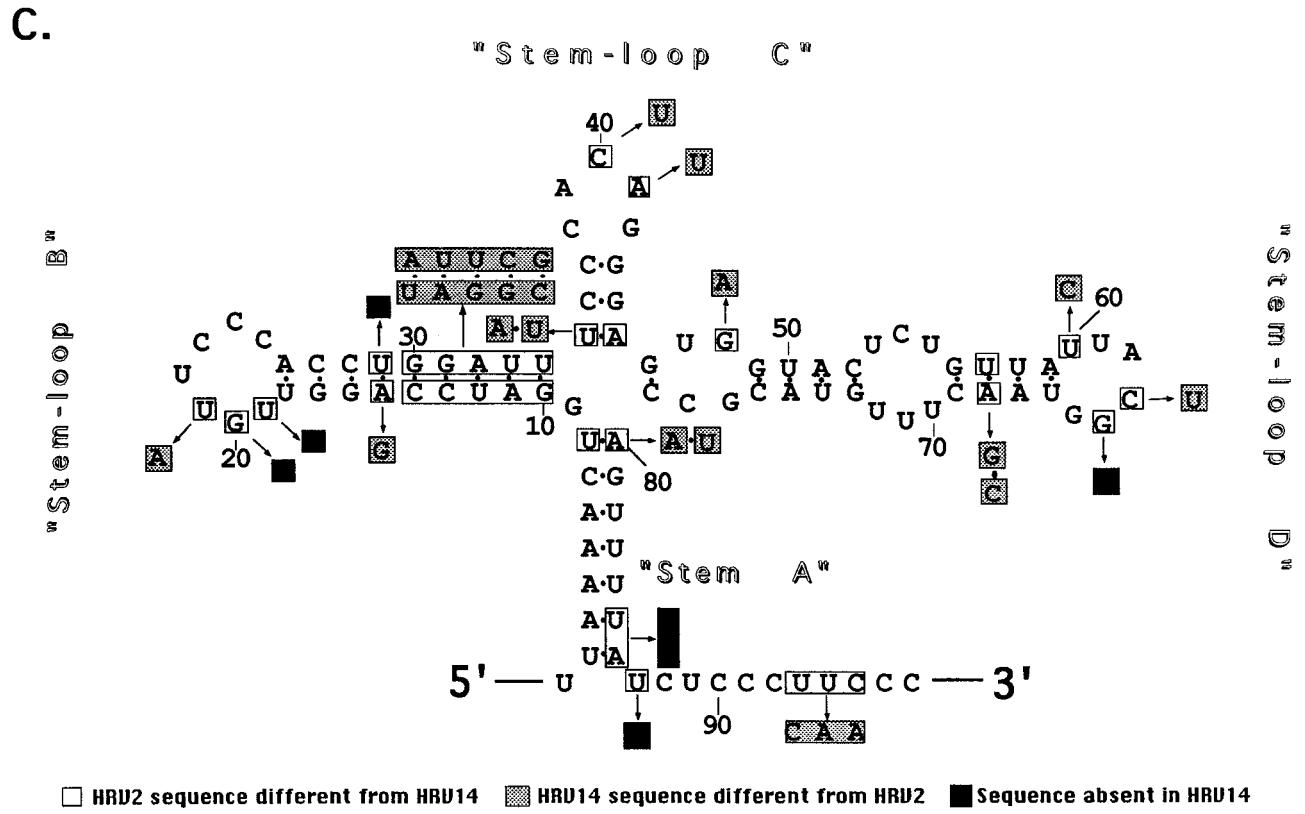


FIG. 2—*Continued.*

(18). The patterns obtained from six different translations (Fig. 4, lanes 3 to 8) were almost identical, an observation suggesting similar translation efficiency and processing events, regardless of the 5′ NTR preceding the PV1(M) ORF. This result also confirmed that all six plasmid constructs encoded an intact ORF for the polyprotein.

**Phenotypic characterization of constructs.** Equal amounts of in vitro-produced RNA transcripts derived from the six plasmids (Fig. 3A) were used to transfect HeLa R19 cell monolayers. After 20 h of incubation at 37°C, cytopathic effects (CPE) were visible in monolayers transfected with PVMS100 transcripts. CPE could be detected in cells at 36, 40, and 48 h after transfection with P100ENPO, R2PIO, and R2ENPO transcripts, respectively. Neither R14PIO nor R14ENPO transcript gave rise to CPE, even after 5 days of incubation.

To determine whether infectious viruses were generated from the RNA transfections, the cell lysates harvested at the time when CPE was most pronounced (20 to 72 h posttransfection) were subjected to plaque assays on R19 HeLa cell monolayers. W1-PVMS100 and W1-P100ENPO yielded large and medium-size plaques, respectively, whereas W1-R2PIO and W1-R2ENPO yielded small plaques (Fig. 3B). In contrast, no infectious virus was detected from cells transfected with R14PIO or R14ENPO RNAs (data not shown). The titer of W1-P100ENPO virus was fourfold lower than that of W1-PVMS100, while titers of W1-R2PIO and W1-R2ENPO viruses were more than 1 log lower in magnitude (Fig. 3A).

Furthermore, all the constructs were analyzed for a possible temperature-sensitive phenotype by RNA transfections and subsequent plaque assays at 32.5 or 39.5°C. The phenotypes at the three temperatures tested here were generally similar for each construct (data not shown). Thus, no temperature-sensitive chimeric virus was recovered.

The plaque phenotypes of either the R2PIO or R2ENPO chimera were generally uniform and stable through four passages of infection (data not shown). The RNAs of either virus extracted from the first and fourth passage were subjected to RNA sequencing of the first 150 nt. No differences from the original HRV2 cloverleaf sequence were observed (data not shown).

In one-step growth experiments, viruses recovered from RNA transfections were used to infect HeLa cells at a multiplicity of infection of 10 (Fig. 5). Compared with PVMS100, the three viable chimeras (P100ENPO, R2PIO, and R2ENPO) were delayed in their initial proliferations. Eventually, virus production in P100ENPO-infected cells reached the wild-type titer, whereas R2PIO- and R2ENPO-infected cells yielded viral titers that were lower by 1 log.

**Analysis of viral RNA replication.** In order to assay the extent of plus-strand RNA synthesis, an [$\alpha$-$^{32}$P]UTP-labeled probe complementary to the 3′ end of the poliovirus genomic RNA was prepared (see Materials and Methods). An RNA dot blot assay using one-half of the total RNA extracted from $10^6$ transfected cells at several time points was performed. As can be seen in Fig. 6A, transcripts of PVMS100 were amplified through the course of transfection. All three viable chimeras showed clearly detectable, albeit lower, levels of genomic RNA replication. At the 0 time point posttransfection, all of the input transcripts (and residual DNA templates) still could be detected by the probe. At 5.5 h posttransfection, however, the signals of the R14PIO- and R14ENPO-related sequences had disappeared. We conclude, therefore, that no detectable plus-

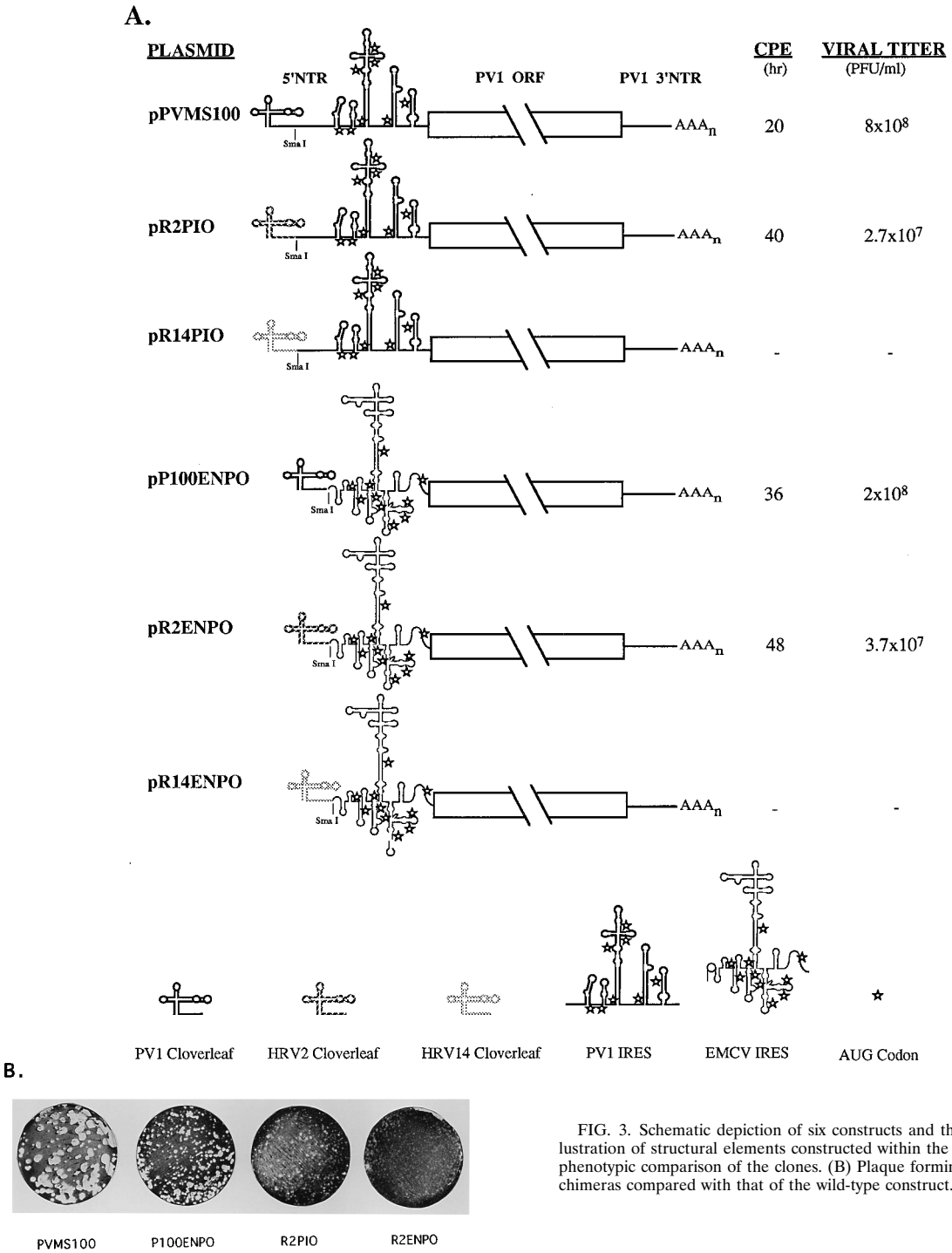


FIG. 3. Schematic depiction of six constructs and their phenotypes. (A) Illustration of structural elements constructed within the 5′ NTRs of clones and phenotypic comparison of the clones. (B) Plaque forming phenotypes of viable chimeras compared with that of the wild-type construct.

sense RNA synthesis occurred in R14PIO- or R14ENPO-transfected cells.

During poliovirus infection, the ratio of viral positive-strand to negative-strand RNAs is, on the average, 50 to 1 (19, 35). The highly sensitive method of reverse transcription-coupled PCR was used to detect negative-sense RNAs. One-tenth of the total RNA extracted from $10^6$ transfected HeLa cells was assayed. To eliminate the DNA templates used for transcription, the RNAs were incubated for 3 h with RNase-free DNase I. To determine if contaminating DNA templates that survived DNase I treatment gave rise to the PCR-amplified products, we analyzed the RNA sample after transfection with PVMS100 transcripts at the 0-h time point. No DNA band was visible on a 1.5% agarose gel, an observation showing that the DNA templates contained in the transcription mixture during transfection were digested by the DNase I to undetectable levels (Fig. 6B, lane 2). Similar results were obtained with other samples at the same time point (data not shown). At 23 h

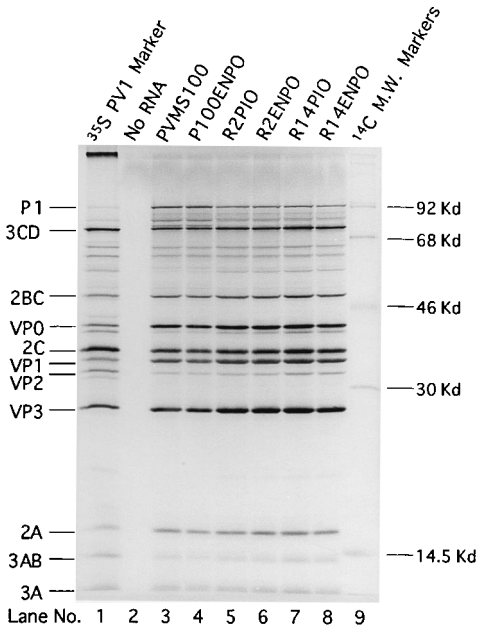


FIG. 4. In vitro protein synthesis and processing directed by the wild-type construct and five chimeras. Equal amounts of in vitro-transcribed RNAs were translated in a HeLa cell extract at 30°C overnight. [$^{35}$S]methionine-labeled PV1(M) proteins extracted from infected HeLa cells were used as markers. M.W., molecular weight.

posttransfection, negative-sense RNA from PVMS100-transfected cells could be easily detected (Fig. 6B, lane 4). In addition, minus-strand RNAs from the three viable constructs could also be detected to a lesser extent (Fig. 6B, lanes 5 to 7). In contrast, no signal was obtained from the total RNA which was extracted from cells at 23 h after transfection with either pR14PIO or pR14ENPO transcript (lanes 8 and 9). These results rule out the possibility that the R14PIO and R14ENPO RNAs are quasi-infectious (reference 5 and references therein). Because of the late time point for the reverse transcription PCR assay, we do not know whether some minus strands were generated shortly after transfection.

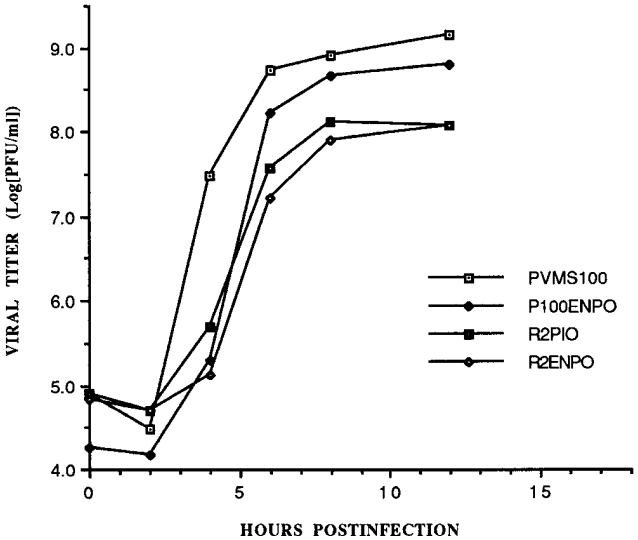


FIG. 5. One-step growth curves of the wild-type construct and three viable chimeras. HeLa cells were infected by viruses at a multiplicity of infection of 10. At various times after infection, cells were harvested and titers of viruses were obtained through plaque assay.

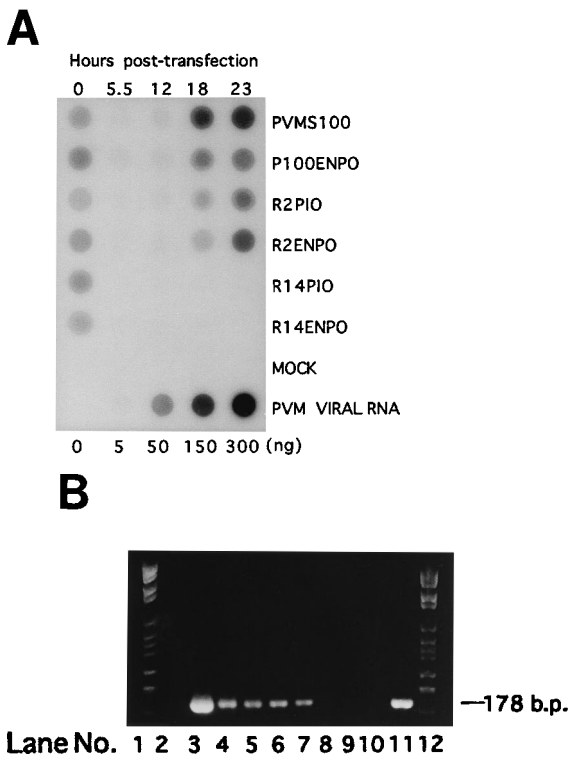


FIG. 6. Detection of RNA syntheses in wild-type transcript- or chimeric transcript-transfected cells. (A) Measurement of plus-strand RNA syntheses by dot blot assay. The bottom panel contained increasing amounts of PV1(M) virion RNAs as controls. (B) Measurement of negative-strand RNA syntheses by reverse transcription-coupled PCR analyses. Ten of 50 μl of total PCR products was loaded. Lanes 1 and 12 contained DNA molecular marker VI (Boehringer Mannheim Co.). Lane 2, detection of negative-strand RNA at 0 h posttransfection; lane 3, detection of plus-strand RNA at 23 h posttransfection for PVMS100; lanes 4 to 10, detection of negative-strand RNAs at 23 h posttransfection for PVMS100, P100ENPO, R2PIO, R2ENPO, R14PIO, R14ENPO, and mock, respectively; lane 11, PCR product with plasmid PVMS100 as template.

**Interactions between cloverleaf RNAs and poliovirus polypeptides 3AB/3CD$^{pro}$.** Two poliovirus-encoded proteins, 3AB and 3CD$^{pro}$ (17), form a tight complex which has been found to specifically recognize the poliovirus 5′-terminal cloverleaf RNA (9). We were interested in determining the extent to which the poliovirus 3AB/3CD$^{pro}$ complex can recognize the cloverleaf from either HRV2 or HRV14. Accordingly, we performed gel shift and competition assays, following protocols recently published by Harris et al. (9).

In the presence of 0.2 μM 3CD$^{pro}$ and 0.8 μM 3AB, the mobility of most of the labeled PVMS100 cloverleaf (20,000 cpm; about 1 nM per reaction) was retarded by the protein complex (Fig. 7A; compare lane 2 with lane 1). This gel shift was apparent even in the presence of a 500 M excess of unlabeled 1A′B or 1A′BC RNA competitor (lanes 4 and 6). However, a 2 M excess of unlabeled 1ABCD RNA (intact cloverleaf) significantly reduced the extent of retardation (lane 7), whereas a 200 M excess of this competitor RNA abolished the shift of the labeled probe (lane 9). 1A′B and 1A′BC RNAs represent the first 34 and 45 nt of the PV1(M) genome, respectively; computer-aided folding analyses predicted that they can maintain stem-loop structures similar to that in the intact cloverleaf. This result is consistent with those obtained by the

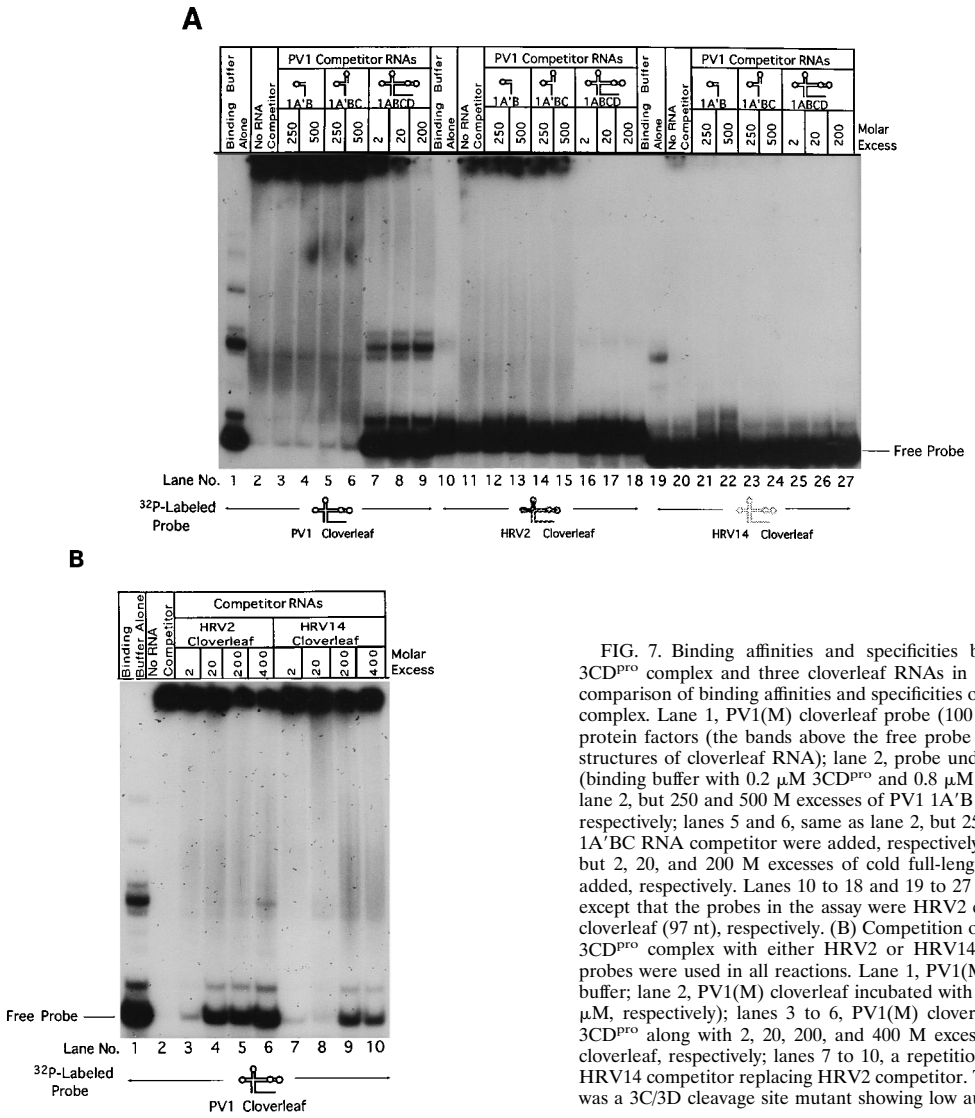


FIG. 7. Binding affinities and specificities between the poliovirus 3AB/3CD$^{pro}$ complex and three cloverleaf RNAs in a gel shift assay. (A) Parallel comparison of binding affinities and specificities of three cloverleaves to protein complex. Lane 1, PV1(M) cloverleaf probe (100 nt) in binding buffer, without protein factors (the bands above the free probe may represent the high-order structures of cloverleaf RNA); lane 2, probe under optimal binding conditions (binding buffer with 0.2 μM 3CD$^{pro}$ and 0.8 μM 3AB); lanes 3 and 4, same as lane 2, but 250 and 500 M excesses of PV1 1A′B RNA competitor were added, respectively; lanes 5 and 6, same as lane 2, but 250 and 500 M excesses of PV1 1A′BC RNA competitor were added, respectively; lanes 7 to 9, same as lane 2, but 2, 20, and 200 M excesses of cold full-length PV1 cloverleaf RNA were added, respectively. Lanes 10 to 18 and 19 to 27 are repetitions of lanes 1 to 9 except that the probes in the assay were HRV2 cloverleaf (98 nt) and HRV14 cloverleaf (97 nt), respectively. (B) Competition of the PV1(M) cloverleaf-3AB/3CD$^{pro}$ complex with either HRV2 or HRV14 cloverleaves. PV1 cloverleaf probes were used in all reactions. Lane 1, PV1(M) cloverleaf probe in binding buffer; lane 2, PV1(M) cloverleaf incubated with 3AB and 3CD$^{pro}$ (0.8 and 0.2 μM, respectively); lanes 3 to 6, PV1(M) cloverleaf incubated with 3AB and 3CD$^{pro}$ along with 2, 20, 200, and 400 M excesses of cold full-length HRV2 cloverleaf, respectively; lanes 7 to 10, a repetition of lanes 3 to 6 but with the HRV14 competitor replacing HRV2 competitor. The purified 3CD$^{pro}$ used here was a 3C/3D cleavage site mutant showing low autoprocessing activity (8).

similar assays reported previously (9). The fact that all binding assays were carried out in the presence of a large (1,000-fold) molar excess of tRNA indicates that the interaction between 3AB/3CD$^{pro}$ complex and full-length cloverleaf is highly specific.

Next, we performed gel shift assays with probes that originated from HRV2 (98 nt) and HRV14 (97 nt). For these experiments, we used the same molar ratios of probes, proteins, and competitors as with the poliovirus cloverleaf. Only a relatively small portion of HRV2 probe could be shifted by the poliovirus 3AB/3CD$^{pro}$ (Fig. 7A; compare lane 11 with lane 10). Significantly, neither the PV1 1A′B nor the 1A′BC RNA influenced the binding between the HRV2 cloverleaf and the poliovirus 3AB/3CD$^{pro}$ (lanes 12 to 15). However, 2 nM 1ABCD competitor RNA completely eliminated the shift of the probe (lane 16). This result demonstrated that a ribonucleoprotein complex could be formed between the polioviral proteins and the HRV2 cloverleaf RNA but that this protein-RNA interaction was weaker than that between the homologous binding partners. In contrast, the HRV14 cloverleaf could hardly be retarded by the poliovirus protein complex (compare lane 20 with lane 19). This interaction could be blocked by adding 1A′B or 1A′BC competitor RNA (lanes 21 to 24), an observation suggesting that the recognition between the poliovirus-encoded proteins and HRV14 cloverleaf RNA is extremely weak.

To confirm the conclusions presented above, unlabeled full-length cloverleaf RNAs from HRV2 and HRV14 were prepared and used as competitors in a gel shift assay (Fig. 7B). Even at a 400 M excess, neither the HRV2 nor the HRV14 competitor RNA could abolish the interaction between the poliovirus probe and 3AB/3CD$^{pro}$ complex (lanes 6 and 10). In contrast, a 2 M excess of the corresponding poliovirus competitor RNA abrogated the association between the poliovirus proteins and either of the rhinovirus cloverleaves (Fig. 7A, lanes 16 and 25). Although the 3AB/3CD$^{pro}$ complex binds to poliovirus cloverleaf RNA with the highest affinity and specificity amongst the three RNA homologs tested, HRV2 competitor RNA, at the level of 20 M excess, can interfere significantly with the gel shift of the poliovirus 3AB/3CD$^{pro}$-cloverleaf complex (Fig. 7B, lane 4), whereas no obvious

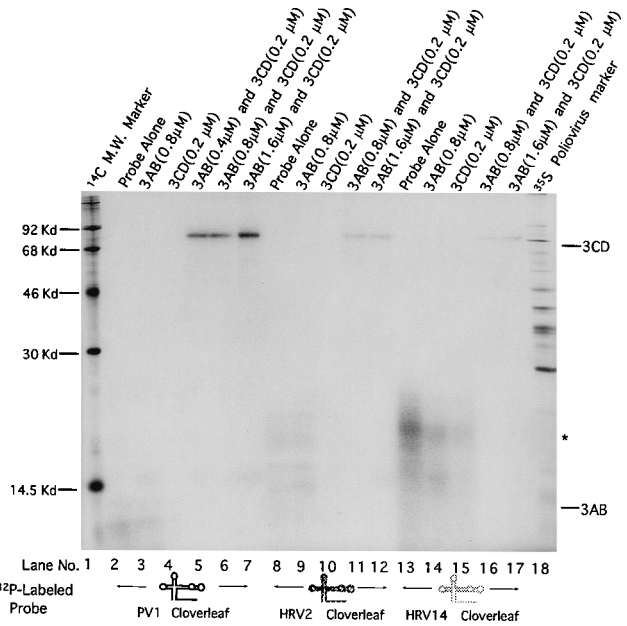


FIG. 8. UV cross-linking of the binding reactions between poliviral 3AB/3CD$^{pro}$ complex and three cloverleaf RNAs. The binding reactions were determined to be identical to the ones in the gel shift assay (except that 20,000 cpm of probe was used in each reaction), and they were then UV cross-linked. The final results were analyzed by SDS–13% PAGE. Lane 1, $^{14}$C molecular weight (M.W.) marker; lanes 2 to 7, PV1(M) cloverleaf used in RNA binding reactions; lanes 13 to 17, HRV14 cloverleaf used in RNA binding reactions; lane 18, [$^{35}$S]methionine-labeled PV1(M) proteins extracted from infected HeLa cells used as markers. *, residual RNA probes that survived RNase digestion.

competition occurred with unlabeled HRV14 probe at the same concentration (lane 8).

We have observed in the past (9) that the 3AB/3CD$^{pro}$-cloverleaf complex is retained at the top of nondenaturing polyacrylamide gels even at low concentrations of 3AB. This phenomenon is apparent also in Fig. 7. 3AB is a highly charged polypeptide with a strong hydrophobic domain that is membrane associated in infected cells (31). The purified protein is soluble only in the presence of detergent (Nonidet P-40), and even then, 3AB has the tendency to form dimers and oligomers (14). We speculate that 3AB may form oligomers large micelles that, in conjunction with the two other binding partners, may prevent migration of the 3AB/3CD$^{pro}$-cloverleaf complex into the gel matrix.

**UV cross-linking assay.** To determine the extent of physical interaction between the poliovirus proteins 3AB/3CD$^{pro}$ and the three cloverleaf homologs, 200,000 cpm of each [α-$^{32}$P]UTP-labeled probe was used to form the protein-RNA complex in the presence of a 1,000 M excess of yeast tRNA as a nonspecific competitor. This was followed by UV cross-linking and RNase digestion. With different concentrations of 3AB present, 3CD$^{pro}$ was labeled strongly by the poliovirus cloverleaf RNA (Fig. 8, lanes 5 to 7) and weakly by the HRV2 cloverleaf (lanes 11 and 12), and at the highest 3AB concentration, it was labeled very weakly by the HRV14 cloverleaf RNA (lanes 16 and 17). Interestingly, very little, if any, 3AB was labeled. In fact, in the presence of tRNA competitor, neither 3AB nor 3CD$^{pro}$ alone could be labeled by any of the cloverleaf probes. These observations suggested that 3AB itself may not interact with [$^{32}$P]UMP-labeled cloverleaf RNA such that a labeled phosphate group can be transferred to the polypeptide chain, whereas a transfer of label to 3CD$^{pro}$ was apparent. Alternatively, 3AB in the 3AB/3CD$^{pro}$-cloverleaf complex does not directly interact with the RNA probe. Experiments to differentiate between these possibilities by labeling the probe with different [α-$^{32}$P]nucleoside triphosphates are in progress. In any event, we consider it possible that 3AB, which complexed with 3CD$^{pro}$, induces a conformational change in the latter that allows the specific interaction with cloverleaf. Overall, the results of the UV cross-linking assay were consistent with those of the gel shift assays, i.e., the poliovirus 3AB/3CD$^{pro}$ complex can bind to its cognate cloverleaf most tightly, whereas the interaction between these proteins and the HRV14 homolog is the weakest.

## DISCUSSION

The genomic RNAs of all enteroviruses and rhinoviruses form 5′-terminal cloverleaf structures (Fig. 2) (28) which have been proposed to function as *cis*-acting elements in genome replication (2, 3, 9, 29). In the present study, we were interested in the dissimilarities rather than the homologies between these picornaviral RNA structures, because they provide naturally occurring variants of a common motif. By constructing poliovirus genomic RNAs containing chimeric 5′ NTRs, we were able to test the functions of different cloverleaves in the context of poliovirus proteins. We have focused on 3AB and 3CD$^{pro}$, the two poliovirus proteins that have been shown recently to form a complex in solution which strongly binds to the cognate 5′-terminal cloverleaf (9, 17). The heterologous cloverleaves chosen were those of HRV2 and HRV14, the former being similar to and the latter quite different from that of poliovirus (Fig. 2).

In addition to the exchange of the cloverleaves, chimeras in which the poliovirus IRES, a type 1 IRES, was replaced with that of EMCV, a type 2 IRES (35), have been constructed. In two cases, this resulted in hybrid picornavirus genomes consisting of genetic elements of three different genera (e.g., HRV cloverleaf-EMCV IRES-poliovirus ORF-3′ NTR). The translation of the corresponding RNA transcripts in HeLa cell extracts revealed translational efficiencies that were almost identical for all six constructs (Fig. 4). This in vitro translation system provides conditions of viral protein synthesis resembling those of the intact cell (18). It is likely, therefore, that the early events of in vivo translation of transcripts transfected into HeLa cells are quite similar for all six constructs, regardless of the composition of the 5′ NTR.

Only transcript RNAs with 5′-terminal cloverleaves of HRV2 and, naturally, of poliovirus were able to produce viruses, regardless of the nature of the adjacent IRES element. This result allows two conclusions. First, the two structural elements, cloverleaf and IRES, appear to function independently from each other in RNA replication and in the initiation of translation, respectively. The construction and viability of dicistronic polioviruses with the gene order poliovirus 5′ NTR-ORF1-EMCV IRES-poliovirus ORF2-3′ NTR (1, 5) support this conclusion. Second, in the context of poliovirus proteins, the cloverleaf of HRV14 does not support RNA replication, a result confirming recent data obtained by Rohll et al. (29) that were published while this study was under way. These results imply that the HRV14 cloverleaf does not assume a structure capable of interacting with poliovirus replication proteins. Alternatively, the HRV14 cloverleaf may assume a nonfunctional higher-order structure in the context of the heterologous RNA. Since in an HRV14 cloverleaf-poliovirus chimera an exchange of structural elements of the HRV14 cloverleaf with elements of poliovirus led to viable virus (29), the latter hypothesis is unlikely. Indeed, our data concerning complex for-

mation between 3AB/3CD$^{pro}$ and cloverleaves strongly support the notion that these poliovirus proteins cannot interact sufficiently strongly with the HRV14 cloverleaf to promote RNA replication.

Andino et al. (2) have recently proposed that the 5′-terminal cloverleaf of poliovirus interacts with a host cellular protein of 36 kDa and that this complex binds the viral proteinase 3CD$^{pro}$. It was postulated that the formation of this complex may be essential for poliovirus genome replication (2). Making use of purified viral protein 3AB, proteinases 3CD$^{pro}$ and 3C$^{pro}$, and polymerase 3D$^{pol}$, Harris et al. (9) have shown that the poliovirus cloverleaf forms a tight complex with 3AB/3CD$^{pro}$, a weak complex with 3AB/3C$^{pro}$, and no complex with 3AB/3D$^{pol}$. These data have led us to the suggestion that, instead of the cellular 36 kDa protein, the viral protein 3AB is likely to be the essential partner in the interaction between 3CD$^{pro}$ and the cloverleaf in the infected cell (9).

The chimeric RNA constructs expressed phenotypes that ranged from medium plaque size to small plaque size as well as a null phenotype (Fig. 3). These phenotypes correlated well with the growth properties of the viral variants (Fig. 5). This offered an opportunity to relate in vivo phenotypic differences to the propensity for complex formation between 3AB/3CD$^{pro}$ and the corresponding cloverleaves. The results of gel shift experiments (Fig. 7) and UV cross-linking (Fig. 8) clearly revealed a tight correlation between the efficiency of formation of the 3AB/3CD$^{pro}$-cloverleaf complex and the ability of the constructs to replicate in vivo. The most plausible interpretation of these results is that the formation of this complex is required for poliovirus RNA replication. This conclusion does not exclude the possibility of the involvement of host factors in this process (see, for example, reference 32). Moreover, other poliovirus nonstructural proteins, e.g., 2A$^{pro}$, 2B, 2BC, 2C, VPg, and 3D$^{pol}$, have been shown to participate in poliovirus RNA replication (35). For example, 3AB binds tightly not only to 3CD$^{pro}$ but also to the RNA polymerase 3D$^{pol}$, and the resulting complex 3AB/3D$^{superpol}$ is 100-fold more active in poly(A)-dependent poly(U) polymerization than 3D$^{pol}$ (14, 20). Whether the fragment (p36) of EF-1α can promote binding of poliovirus 3CD$^{pro}$ to the HRV14 cloverleaf or whether HRV14 3AB/3CD$^{pro}$ can bind to the poliovirus cloverleaf will be the subject of a separate study. Numerous details of the functions of the poliovirus nonstructural proteins in genome replication remain to be elucidated.

## ACKNOWLEDGMENTS

We thank Günter Bernhardt and Aniko Paul for constructive suggestions and valuable technical advice. We are especially thankful to Aniko Paul and Andy Cuconati for purified 3AB and HeLa cell translation extract, respectively.

W.X. is a member of the graduate training program in biochemistry and cell biology. K.S.H. and L.A. were members of graduate training programs in molecular genetics and microbiology and in genetics, respectively.

This work was supported in part by grants PN9329 (HFSPO), AI15122, and AI32100.

## REFERENCES

1. **Alexander, L., H. H. Lu, and E. Wimmer.** 1994. Polioviruses containing picornavirus type 1 and/or type 2 internal ribosomal entry site elements: genetic hybrids and the expression of a foreign gene. Proc. Natl. Acad. Sci. USA **91:**1406–1410.
2. **Andino, R., G. E. Rieckhof, P. L. Achacoso, and D. Baltimore.** 1993. Poliovirus RNA synthesis utilizes an RNP complex formed around the 5′-end of viral RNA. EMBO J. **12:**3587–3598.
3. **Andino, R., G. E. Rieckhof, and D. Baltimore.** 1990. A functional ribonucleoprotein complex forms around the 5′ end of poliovirus RNA. Cell **63:**369–380.
4. **Andino, R., G. E. Rieckhof, D. Trono, and D. Baltimore.** 1990. Substitutions in the protease (3C$^{pro}$) gene of poliovirus can suppress a mutation in the 5′ noncoding region. J. Virol. **64:**607–612.
5. **Cao, X., and E. Wimmer.** Intragenomic complementation of a 3AB mutant in dicistronic polioviruses. Virology, in press.
6. **Cao, X. M., R. J. Kuhn, and E. Wimmer.** 1993. Replication of poliovirus RNA containing two VPg genes leads to a specific deletion event. J. Virol. **67:**5572–5578.
7. **Harris, K. S., C. U. T. Hellen, and E. Wimmer.** 1990. Proteolytic processing in the replication of picornaviruses. Semin. Virol. **1:**323–333.
8. **Harris, K. S., S. R. Reddigari, M. J. H. Nicklin, T. Hämmerle, and E. Wimmer.** 1992. Purification and characterization of poliovirus polypeptide 3CD, a proteinase and a precursor for RNA polymerase. J. Virol. **66:**7481–7489.
9. **Harris, K. S., W. Xiang, L. Alexander, A. V. Paul, W. S. Lane, and E. Wimmer.** 1994. Interaction of the polioviral polypeptide 3CD$^{pro}$ with the 5′ and 3′ termini of the poliovirus genome: identification of viral and cellular cofactors necessary for efficient binding. J. Biol. Chem. **269:**27004–27014.
10. **Jang, S. K., M. V. Davies, R. J. Kaufman, and E. Wimmer.** 1989. Initiation of protein synthesis by internal entry of ribosomes into the 5′ nontranslated region of encephalomyocarditis virus RNA in vitro. J. Virol. **63:**1651–1660.
11. **Jang, S. K., H.-G. Kräusslich, M. J. H. Nicklin, G. M. Duke, A. C. Palmenberg, and E. Wimmer.** 1988. A segment of the 5′ nontranslated region of encephalomyocarditis virus RNA directs internal entry of ribosomes during in vitro translation. J. Virol. **62:**2636–2643.
12. **Kuhn, R. J., H. Tada, M. F. Ypma-Wong, B. L. Semler, and E. Wimmer.** 1988. Mutational analysis of the genome-linked protein VPg of poliovirus. J. Virol. **62:**4207–4215.
13. **Kunkel, T. A.** 1985. Rapid and efficient site-specific mutagenesis without phenotypic selection. Proc. Natl. Acad. Sci. USA **82:**488–492.
14. **Lama, J., A. V. Paul, K. S. Harris, and E. Wimmer.** 1994. Properties of purified recombinant poliovirus protein 3AB as substrate for viral proteinases and as co-factor for viral polymerase 3D$^{pol}$. J. Biol. Chem. **269:**66–70.
15. **Larsen, G. R., B. L. Semler, and E. Wimmer.** 1981. Stable hairpin structure within the 5′ terminal 85 nucleotides of poliovirus RNA. J. Virol. **37:**328–335.
16. **Lawson, M. A., and B. L. Semler.** 1992. Alternate poliovirus nonstructural protein processing cascades generated by primary sites of 3C proteinase cleavage. Virology **191:**309–320.
17. **Molla, A., K. S. Harris, A. V. Paul, S. H. Shin, J. Mugavero, and E. Wimmer.** 1994. Stimulation of poliovirus proteinase 3C$^{pro}$-related proteolysis by the genome-linked protein VPg and its precursor 3AB. J. Biol. Chem. **269:**27015–27020.
18. **Molla, A., A. V. Paul, and E. Wimmer.** 1991. Cell-free, de novo synthesis of poliovirus. Science **254:**1647–1651.
19. **Novak, J. E. K., and K. Kirkegaard.** 1991. Improved method for detecting negative strands used to demonstrate specificity of plus-strand encapsidation and the ratio of positive to negative strands in infected cells. J. Virol. **65:**3384–3387.
20. **Paul, A., X. Cao, K. S. Harris, and E. Wimmer.** 1994. Studies with poliovirus polymerase 3D$^{pol}$: stimulation of poly(U) synthesis in vitro by purified poliovirus protein 3AB. J. Biol. Chem. **269:**29173–29181.
21. **Paul, A. V., A. Molla, and E. Wimmer.** 1994. Studies of a putative amphipathic helix in the N-terminus of poliovirus protein 2C. Virology **199:**188–199.
22. **Pelletier, J., and N. Sonenberg.** 1988. Internal initiation of translation of eukaryotic mRNA directed by a sequence derived from poliovirus RNA. Nature (London) **334:**320–325.
23. **Pelletier, J., and N. Sonenberg.** 1989. Internal binding of eucaryotic ribosomes on poliovirus RNA: translation in HeLa cell extracts. J. Virol. **63:**441–444.
24. **Pilipenko, E. V., V. M. Blinov, L. I. Romanova, A. N. Sinyakov, S. V. Maslova, and V. I. Agol.** 1989. Conserved structural domains in the 5′-untranslated region of picornaviral genomes: an analysis of the segment controlling translation and neurovirulence. Virology **168:**201–209.
25. **Pilipenko, E. V., S. V. Maslova, A. N. Sinyakov, and V. I. Agol.** 1992. Towards identification of cis-acting elements involved in the replication of enterovirus and rhinovirus RNAs: a proposal for the existence of tRNA-like terminal structures. Nucleic Acids Res. **20:**1739–1745.
26. **Racaniello, V. R., and C. Meriam.** 1986. Poliovirus temperature-sensitive mutant containing a single nucleotide deletion in the 5′-noncoding region of the viral RNA. Virology **155:**498–507.
27. **Reuer, Q., R. J. Kuhn, and E. Wimmer.** 1990. Characterization of poliovirus clones containing lethal and nonlethal mutations in the genome-linked protein VPg. J. Virol. **64:**2967–2975.
28. **Rivera, V. M., J. D. Welsh, and J. V. Maizel.** 1988. Comparative sequence analysis of the 5′ noncoding region of the enteroviruses and rhinoviruses. Virology **165:**42–50.
29. **Rohll, J. B., N. Percy, R. Ley, D. J. Evans, J. F. Almond, and W. S. Barclay.** 1994. The 5′-untranslated regions of picornavirus RNAs contain independent functional domains essential for RNA replication and translation. J. Virol. **68:**4384–4391.
30. **Rueckert, R. R.** 1990. Picornaviridae and their replication, p. 507–548. *In*

B. N. Fields, D. M. Knipe, R. M. Chanock, M. S. Hirsch, J. L. Melnick, T. P. Morath, and B. Roizman (ed.), Virology, 2nd ed., vol. 1. Raven Press, New York.

31. **Semler, B., C. Anderson, R. Hanecak, L. Dorner, and E. Wimmer.** 1982. A membrane-associated precursor to poliovirus VPg identified by immunoprecipitation with antibodies directed against a synthetic heptapeptide. Cell **28:**405–412.
32. **Shiroki, K., H. Kato, S. Koike, T. Odaka, and A. Nomoto.** 1993. Temperature-sensitive mouse cell factors for strand-specific initiation of poliovirus RNA synthesis. J. Virol. **67:**3989–3996.
33. **Simoes, E., and P. Sarnow.** 1991. An RNA hairpin at the extreme 5′ end of the poliovirus RNA genome modulates viral translation in human cells. J. Virol. **65:**913–921.
34. **Werf, S. V. D., J. Bradley, E. Wimmer, F. W. Studier, and J. J. Dunn.** 1986. Synthesis of infectious poliovirus RNA by purified T7 RNA polymerase. Proc. Natl. Acad. Sci. USA **83:**2330–2334.
35. **Wimmer, E., C. U. T. Hellen, and X. M. Cao.** 1993. Genetics of poliovirus. Annu. Rev. Genet. **27:**353–436.